Size Dependence of the Dissolution of ZnO Nanoparticles

Eric A. Meulenkamp†

Philips Research Laboratories Eindhoven, Prof. Holstlaan 4 (WA13), 5656 AA Eindhoven, The Netherlands

Received: May 19, 1998; In Final Form: July 14, 1998

ZnO nanoparticles of about 30−60 Å size in ethanolic solution were etched by addition of anhydrous acetic acid. Upon dissolution, the volume-weighted particle size decreased by about 10%. The polydispersity increased slightly. The dissolution rate was strongly dependent on particle size, and size selective etching of a mixture of ZnO particles was demonstrated. The change of the particle size during etching can be modeled adequately by a Monte Carlo simulation, in which the known degree of polydispersity and the size dependence of the etch rate are taken into account. On the basis of a comparison with work on the dissolution of silica nanoparticles and oxidic thin films, and on the etching of single-crystal ZnO, it is proposed that the size dependence is caused by variations of the chemical reactivity of the nanoparticles related to, for example, the concentration of defects and kink sites. Thus, dissolution provides a convenient method to investigate size-dependent chemical properties.

1. Introduction

Nanocrystalline materials currently receive much attention as they represent a class of materials which promises new properties and products, and new processing paths. A well-studied example is the nanocrystalline TiO_2 solar cell, developed by Grätzel and co-workers.[1] The huge surface area associated with the use of a nanoparticulate porous electrode is used to obtain a large volume concentration of an adsorbed organic dye which can efficiently harvest sunlight.

The properties of nanocrystalline materials have been characterized extensively using, for example, optical spectroscopy and electrical or magnetic measurements. Relatively little attention has been paid to their wet-chemical properties, and the possible size dependence thereof. For example, it is not yet clear if the colloid-chemical stability can be described accurately by the classical DLVO theory. This work investigates the chemical etching, or dissolution, of nanoparticles. ZnO was chosen because it is used in several industrial applications[2] and because it can serve as a representative example of the important class of oxidic nanoparticles. It also shows quantum confinement effects for particle sizes $\lesssim$60 Å.[3] Thus, optical absorption measurements can be used to obtain the ZnO concentration and particle size, using a calibration graph of size vs optical band gap.[4]

Etching of nanoparticles has been discussed in previous works. Two groups independently reported on the selective photodissolution of CdS nanoparticles.[5,6] By tuning the incoming light in the longer wavelength region of the optical absorption, selective absorption by larger particles was achieved. Dissolution of the particles was accomplished by the action of the photogenerated holes. Indeed, this technique can be used to tune the size of the particles to a desired value and to decrease polydispersity, albeit at the expense of particle concentration and the presence of dissolution products in solution. Whetten[7] has discussed selective etching of particles on the basis of differences in their chemical reactivity due to, for example, variations in defect density and surface faceting. These ideas were based on experimental evidence obtained using gas-phase reactions of clusters. As far as we are aware, no work along these lines has been reported using wet-chemical processing.

This work describes chemical etching of ZnO nanoparticles. It can be used to decrease the particle size, similar to what was reported for photodissolution. Size-selective etching of ZnO is also demonstrated. It is argued that this is probably due to the type of selectivity discussed by Whetten. It emerges that a closer look at the evolution of particle size and particle concentration during etching can give interesting information on nanoparticle properties, not readily obtainable by other techniques.

2. Experimental Section

ZnO was prepared according to the method developed by Spanhel and Anderson,[8] with a few modifications described earlier.[4] Briefly, 1.10 g (5 mmol) $Zn(Ac)_2 \cdot 2H_2O$ (Aldrich) was dissolved in 50 mL boiling absolute ethanol (Merck, p.A.), and cooled to 0 °C. Then, 0.29 g (7 mmol) $LiOH \cdot H_2O$ was dissolved in 50 mL ethanol at room temperature, cooled to 0 °C and slowly added to the Zn(II) solution under vigorous stirring. The reaction mixture was stored at $\approx$4 °C. The desired particle size (25 Å $\lesssim$ size $\lesssim$70 Å) was obtained by aging the ZnO sol at 4 °C or at room temperature. The sols were not washed,[4] *i.e.*, cleaned of acetate and water. The effects of Ac^- and H_2O were studied by their addition to the as-prepared sol.

Glacial acetic acid, bromine, iodine, and hydrogen peroxide (p.A. quality) were all from Merck. Optical absorption spectra were recorded on a Perkin−Elmer Lambda 19 spectrophotometer. Etch rate experiments were carried out using a thermostated cuvette holder. The reactants were mixed inside the thermostated cuvette. The ZnO concentration in the reaction mixture was typically 2.5 mM at the start of the experiment.

3. Results

3.1 ZnO Etchants. ZnO can be regarded as a complexed form of Zn(II). Thus, addition of complexing agents stronger than oxygen can induce dissolution of ZnO to give $Zn(L^{z-})_n^{(2-nz)+}$ (where L represents the ligand) and H_2O/OH^-. Poly(ethyleneimine) and EDTA addition indeed resulted in ZnO dissolution. However, the etch rate was too fast to be measured accurately, and this type of etchant was not pursued further.

It was found that strong oxidizing agents (H_2O_2, I_2, Br_2) were also capable of ZnO dissolution. At first sight, this is unexpected because some of these are not capable of etching single-crystal ZnO in aqueous solutions. It was noted that the action of these etchants was accompanied by a pH decrease. This is ascribed to oxidation of the solvent and to the well-

† E-mail: meulenka@natlab.research.philips.com.

S1089-5647(98)02305-0 CCC: $15.00
Published on Web 09/16/1998

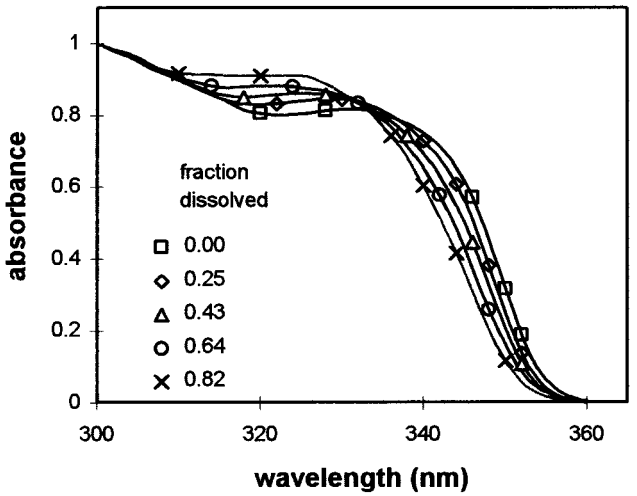

Figure 1. Optical absorption spectra (absorbance at 300 nm set at 1.0) of ZnO sols to which various amounts of HAc were added at −18 °C. The spectra were obtained after completion of the reaction at −18 °C. The legend indicates the fraction of ZnO dissolved, calculated on the basis of the absorption at 300 nm.

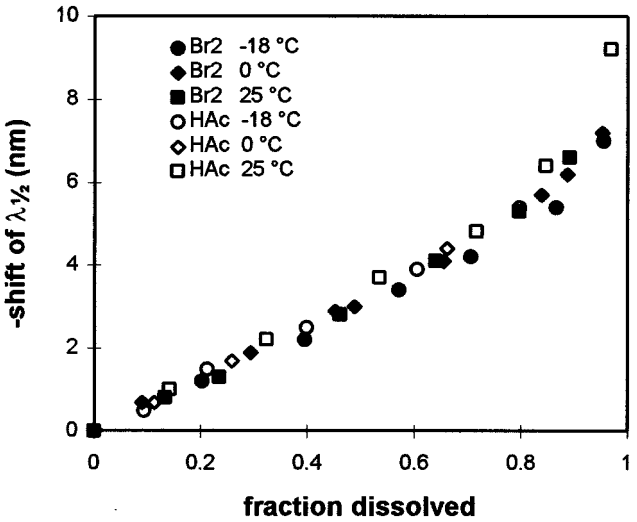

Figure 2. Shift of the absorption spectrum, denoted by $\lambda_{1/2}$, induced by HAc or Br_2 addition at three temperatures. The fraction of ZnO dissolved was determined by the relative absorption at 300 nm. $\lambda_{1/2}$ of the original sol was 349 nm.

known disproportionation reaction of halogens at high pH, which consumes hydroxyl ions. The acids formed can react with ZnO as follows:

$$ZnO + 2HX \rightarrow Zn^{2+} + 2X^{-} + H_2O \qquad (1)$$

Here, X represents the anion present. The oxidizing agents were not studied in detail. The reasons for this are the following. Addition of H_2O_2 without simultaneous addition of water was not possible since H_2O_2 was available only as a 30% aqueous solution. Water plays an important role in ZnO reactivity (see below and ref 4) and its concentration should be constant in all experiments. The sol was also more sensitive to flocculation at the higher water content, which prevented accurate absorption measurements. Iodine and bromine both show strong optical absorption in the visible and UV region, and ZnO absorption measurements are then only possible after completion of the reaction. Some results obtained with Br_2 are discussed below for the sake of comparison.

A third way to dissolve ZnO is to lower the pH by addition of acid. Actually, this turned out to be the most suitable etching technique. Glacial acetic acid (HAc) was used throughout this work because it is the only common acid which is virtually water-free and because it does not introduce new species in the ZnO sol as an acetate salt is used in the synthesis. Note that other organic acids can also be used. It was found that dissolution induced by HAc addition was sufficiently slow such that local concentration variations present during mixing of the reactants did not affect the experiments. Results obtained by addition of HAc to ZnO sol or vice versa were identical within experimental error.

3.2. Particle Size Decrease. The effect of etching on ZnO particle size was studied in two sets of experiments. ZnO dissolved completely when an amount of HAc was added equal to the amount of LiOH used in the synthesis. One set used a quantity of HAc too small to dissolve all ZnO. After completion of the reaction, the absorption spectrum was measured. An example is given in Figure 1. The absorbance for each curve at 300 nm (A_{300}) has been set at 1.0 to illustrate the spectral changes observed. The shape of the spectrum in the wavelength region between about 260 and 310 nm did not change upon ZnO dissolution. A_{300} was also found to be relatively independent of particle size in aging experiments.[4] Hence, A_{300} is a measure of the fraction of ZnO left intact.

The most important aspect of Figure 1 is the clear shift of the onset of the ZnO band gap absorption to lower wavelengths upon dissolution. This is a manifestation of the quantum size effect since an increase in the ZnO optical band gap is found for particle sizes $\lesssim$60 Å.[3] In a previous work[4] we established the relationship between the volume-weighted size D (Å) and $\lambda_{1/2}$ (nm). $\lambda_{1/2}$ was defined as the wavelength at which the absorption was 50% of that at the excitonic peak (or shoulder). The relationship, which is valid for 25 Å $< D <$ 65 Å, was given by $1240/\lambda_{1/2} = 3.556 + 799.9/D^2 - 22.64/D$. The absorption shift shown in Figure 1 corresponds to a size decrease from approximately 35.2 to 32.5 Å. The increase of the absorption in the wavelength region from about 310 to 333 nm should also be noted. It is caused by the formation of smaller particles with a higher absorption in this region. The overall shape of the absorption indicates a small increase in polydispersity as more ZnO dissolves.

It is important at this point to consider whether the results shown in Figure 1 are unique to the combination of etchant and temperature. Figure 2 shows results for two etchants, HAc and Br_2, at three temperatures. Data shown are the shift of the $\lambda_{1/2}$ values, measured after completion of the reaction, versus the fraction of ZnO dissolved. Obviously, there is no significant effect of temperature or etchant on the shift of the absorption spectrum. The shape of the absorption spectrum was independent of the etchant used. These results also point out that the etch rate has no influence on the ZnO particle size at a particular fraction of ZnO left intact. For example, the reaction of Br_2 at −18 °C took several hours, whereas reaction with HAc at 20 °C was complete in a few minutes. It is concluded that results obtained with HAc are representative for the size evolution during ZnO etching.

The results presented above were obtained after completion of the reaction. In a second set of experiments spectra were recorded during etching. The conditions were chosen such that the error introduced by continued etching during recording was small (recording time < 20 s). A typical experiment required about 30 min. Results for three ZnO sols are collected in Figure 3. The $\lambda_{1/2}$ values were converted into particle size as described earlier. Note the logarithmic x-axis describing the fraction of ZnO left intact. The particle-size decrease is rather limited and

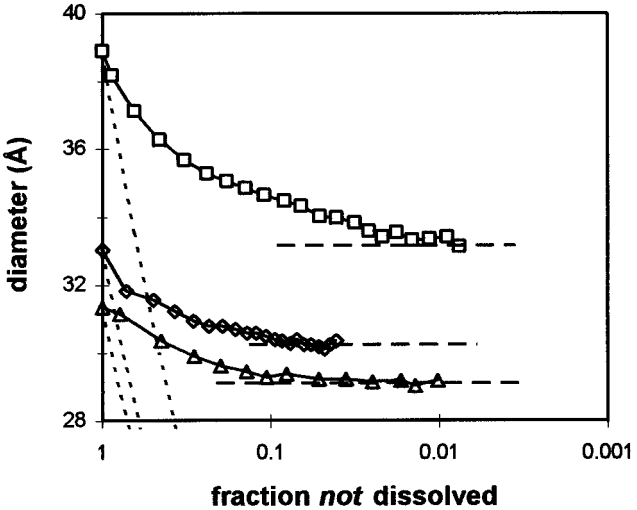

Figure 3. ZnO particle-size evolution during etching by HAc measured for three sols at 0 °C The size was determined from the optical band gap ($\lambda_{1/2}$). Note the logarithmic *x*-axis describing the fraction of ZnO not dissolved. The dashed lines indicate the apparent lower limit of the particle size. The dotted lines describe the cube-root dependence discussed in the text.

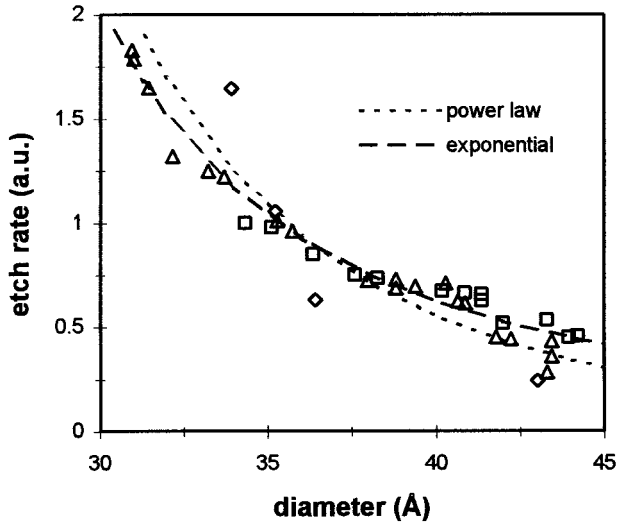

Figure 4. Size dependence of the etch rate, defined as the initial rate of decrease of the amount of ZnO, for three ZnO sols at 25 °C. The etch rates of sol no. 2 (◇) and 3 (△) were multiplied by 0.55 and 0.8, respectively. The dashed lines show an exponential and a power law dependence.

amounts to about 10%. A cube-root dependence of the diameter on the amount, or volume, of ZnO can be expected if each particle is etched at the same rate: $D/D_{\text{initial}} = f^{1/3}$, where f is the fraction not dissolved. This model corresponds to a picture where ZnO is gradually "peeled off" all particles at the same rate. It is indicated by the dotted lines. Such a simple model clearly does not describe the experimental results and the decrease of the particle *size* is much smaller than predicted. This implies that the *number* of particles decreases substantially already during the early stages of etching. Another interesting feature is the almost constant particle size when more than about 90% of the ZnO has dissolved. In other words, the particle size decreases slowly until an apparent limit is reached, indicated by the dashed lines in Figure 3, below which, effectively, only the *number* of particles appears to decrease.

3.3 Size Selective Etching. Possible size selective etching was studied by investigating the rate of dissolution of ZnO sols of various sizes. Figure 4 shows the size dependence of the etch rate for three ZnO sols, which were produced in three

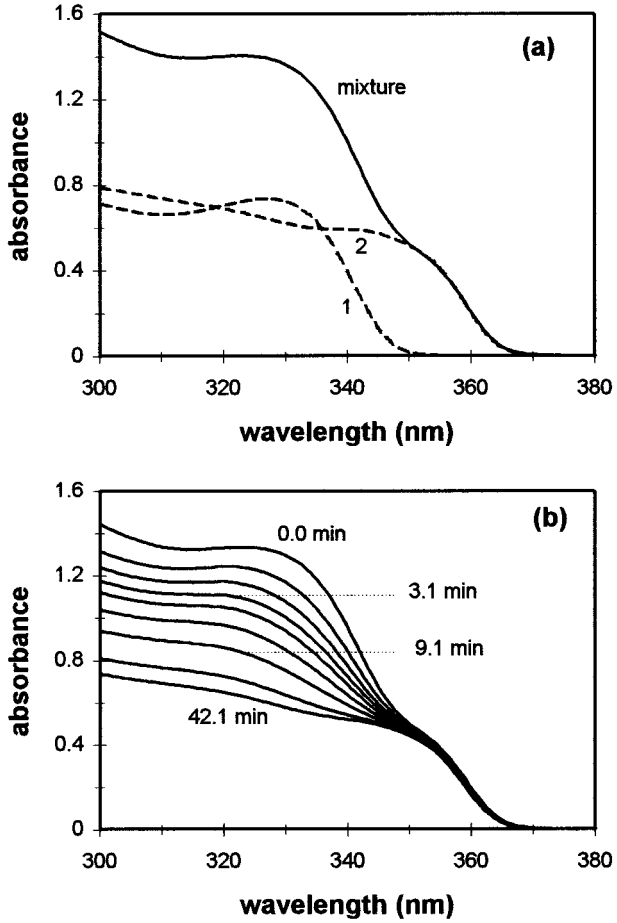

Figure 5. Evolution of the absorption spectrum of a mixture of two ZnO sols upon addition of HAc at 0 °C. The $\lambda_{1/2}$ values of the original sols were about 342 and 358 nm. Their absorption spectra, and that of the mixture, are shown in (a). The spectra measured during etching are shown in (b). The time elapsed after HAc addition is indicated.

separate synthesis runs. The etch rate was defined as the initial rate of the decrease of the ZnO absorption with time (see also Section 3.4). It can be clearly seen that the etch rate depends markedly on the particle size. For example, the rate found for 43 Å particles was about 5 times smaller than that for 30 Å particles. The dashed lines show arbitrary power law and exponential relationships (see Discussion) which can describe the observed size dependence.

The size dependence of the etch rate could only be studied properly using sols derived from a single synthesis run, after which the size was varied by aging. Although the size dependencies of the etch rates of sols produced in several synthesis runs are in agreement, the absolute values of the etch rates at a particular particle size could differ by a factor of about three. The multiplication factor indicated in Figure 4 illustrates this point: Sol 2 (◇) showed an etch rate approximately 1.8 times higher than the other sols.

It is conceivable that during aging not only the particle size changes, but also other parameters which can affect the etch rate, such as the pH. Therefore, an additional experiment was carried out. Approximately equal amounts of ZnO with about 31.5 and 43 Å size were mixed, with $\lambda_{1/2}$ values of 342 and 358 nm, respectively. The sols were derived from the same synthesis run. Their absorption spectra, and that of the mixture, are given in Figure 5a. HAc was added to dissolve about 50% of the ZnO. Spectra were recorded during dissolution. These are shown in Figure 5b. It is obvious that the smaller particles react much faster, in accordance with Figure 4. The final

spectrum shows that about 90% of the 31.5 Å ZnO has reacted, while only 15% of the 43 Å particles has dissolved. Thus, the observed size dependence is not due to variations of parameters other than the ZnO size and it is possible to selectively etch the smaller particles.

3.4 Kinetics of Etching. To compare the etch rates in a more quantitative way, elucidation of the kinetics of the etching process would be very useful. Several experiments were carried out using excess amounts of reactants, in terms of the dissolution reaction of eq 1, up to a factor of about five. The absorption transients were fitted to simple kinetic rate laws. For example, the etch rate can be expressed as the initial rate of dissolution. This is used in Figure 4:

$$-(\mathrm{d[ZnO]}/\mathrm{d}t)_{\mathrm{initial}} = k_1[\mathrm{ZnO}]_0^{\,a}[\mathrm{HAc}]_0^{\,b} \qquad (2)$$

where k is a rate constant, the subscript 0 refers to time $t = 0$, and the superscripts a and b are the reaction orders. Using an excess of HAc, its concentration can be considered constant and a pseudo-first-order rate law is obtained by assuming $a = 1$:

$$-(\mathrm{d[ZnO]}/\mathrm{d}t) = k_2[\mathrm{ZnO}] \qquad (3)$$

Although we had some success in analyzing a number of absorption transients using eqs 2−3 and analogous equations, it was not possible to obtain a consistent description for all etch conditions used. For example, the initial rate equation and the pseudo-reaction order equation yielded reaction orders for HAc between 2.0 and 2.7. The inability to describe the kinetics in detail is not surprising if one considers the changes in the solution composition during etching. The particle size D varies. Since the etch rate can be expected to depend on D, this, and polydispersity, should be accounted for in a complete description. The activities of HAc and H^+ are unknown and vary during etching according to pH measurements. It is interesting to note, in this respect, the work by Gerischer and Sorg on dissolution of well-characterized single-crystal ZnO.[9] They also concluded that it was not possible to set up a quantitative model to describe the dissolution kinetics.

Hence, the kinetics of etching were not investigated in detail. Care was taken to compare experiments using identical ZnO and HAc concentrations only. Figures 4−6 are examples of such experiments. The concentration of other components in the reaction mixture (H_2O and LiAc) is also important. These components originate from the chemicals used for the ZnO synthesis. It was found that the etch rate doubled as 1.0 vol % H_2O was added to the reaction mixture. Addition of 100 mM LiAc resulted in a 5-fold increase in the etch rate. Note, however, that these concentrations did not vary in comparative experiments since the same concentrations of ZnO sol were used throughout.

All comparative experiments were carried out under thermostated conditions. Figure 6a shows the temperature dependence of the etch rate found for a large excess of HAc. It provides an example of conditions where a rather good fit to pseudo-first-order kinetics (eq 3) is observed for a 2 orders of magnitude variation of the amount of ZnO. The rate constants follow the Arrhenius rate law (see Figure 6b). The activation energy is about 38 kJ mole^{-1}.

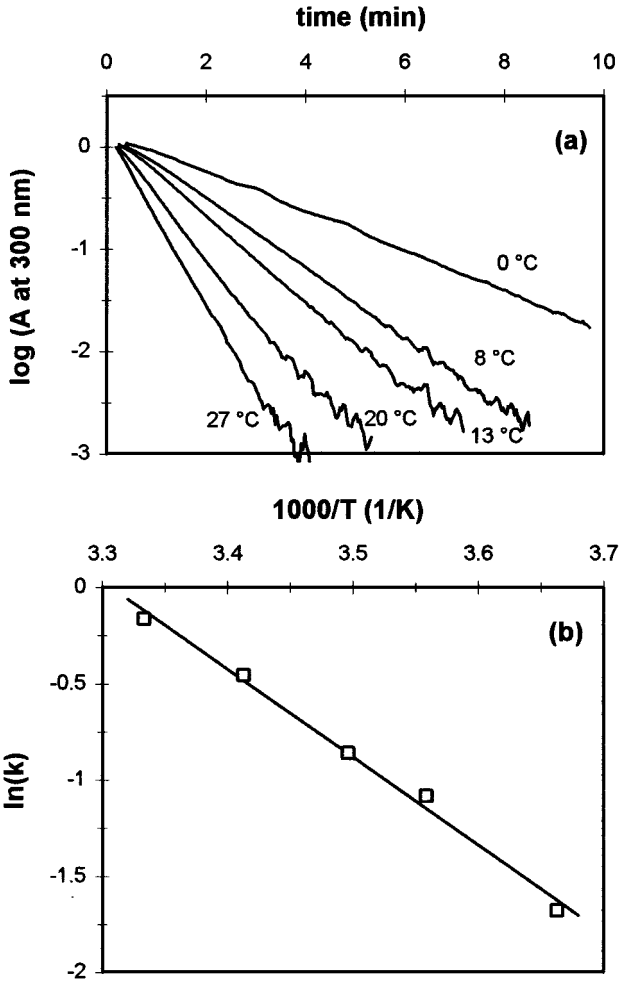

Figure 6. Effect of temperature on the ZnO etch rate using a large excess of HAc. (a) shows the absorption−time transients plotted according to eq 3. (b) is an Arrhenius plot of the rate constants derived from (a).

4. Discussion

4.1. General Description. We set out to discuss a few general findings which relate to previous work on ZnO dissolution and dissolution characteristics of some other oxides. Gerischer and Sorg studied the dissolution of single-crystal ZnO.[9] They found an activation energy of the etch rate, independent of crystal face, of about 45 kJ mole^{-1}, in agreement with the present result. Such a value is typical for a kinetically limited dissolution reaction. The (extrapolated) etch rate found in ref 9 was of the order of 10^{-10} and 10^{-8} mole cm^{-2} h^{-1} at pH = 8, in the absence and presence of acetate, respectively. This pH is close to the isoelectric point, a situation also encountered here. We observed that the experimentally found initial etch rate of 5 nm particles was equivalent to complete dissolution in about 20 min. This corresponds to an etch rate of 2×10^{-8} mole cm^{-2} h^{-1}. The very close agreement with Gerischer and Sorg must be considered fortuitous, as the effects of solvent (ethanol vs water), HAc concentration, and particle size were not fully taken into account. Nevertheless, the roughly similar etch rates underline the good crystallinity of ZnO nanoparticles[3,4,8] and lend support to a further comparison with ZnO single-crystal data.

One of the conclusions in ref 9 was that (complexing) anions such as acetate have a marked influence on the etch rate induced by a pH decrease. This is in good agreement with the present results. They also noted that the nature of the anion, e.g. NO_3^-, ClO_4^-, or Cl^-, affects the etch rate. This underlines the suitability of HAc as etchant in our work since it does not introduce new anions to the reaction mixture.

It is interesting, at this point, to reflect on the implications of these results for the *growth*, or aging, of ZnO. It was argued[4]

that soluble Zn^{II} species and the dissolution and condensation reactions play an important role in this process. H_2O and acetate were found to accelerate aging. It was not possible to distinguish between acceleration of the dissolution and the condensation reactions. Here, it is observed that both species affect the etch rate in a manner consistent with their effect on aging. The addition of Cl^- also resulted in much faster etching, in accordance with its effect on the rate of aging. Finally, although addition of a small amount of acid can slow aging considerably,[4] a steady-state situation in which no net aging or dissolution takes place appears not feasible. This is due to the large difference in rates of these processes (days vs minutes) and the increase in the rate of aging in the presence of reaction products (acetate, zinc).

The merit of etching is probably not in the preparation of ZnO particles of a particular size because the size decrease obtained is relatively small (see Figure 3), especially in comparison with photodissolution,[5,6] but in its use as a characterization method. Growth and dissolution are based on the same kind of hydrolysis/condensation reactions, and etch studies may provide valuable clues about the parameters that govern the rate of growth of nanoparticles. The scatter found when the etch rates of sols obtained in various synthesis runs were compared may also be an important aspect. It is possibly related to small variations in water content or to differences in crystallinity, defect concentration, surface groups, faceting, etc.

Indeed, the surface treatment determined the initial etch rate of single-crystal ZnO.[9] O'Connor and Greenberg studied the dissolution behavior of several types of silica[10] with various levels of impurities and hydration. They concluded that different silicas can actually be characterized by their solubility and etching kinetics. It appears that most work on dissolution of small particles was done using silica,[11] although HF etching has recently been used to increase the band gap photoluminescence efficiency of InP quantum dots.[12] This was attributed to removal of surface recombination centers. Etching has also been used to characterize properties of oxidic thin films. The relative degree of condensation of sol−gel derived films of TiO_2 and SiO_2 was obtained from etch rate measurements in dilute HF.[13] The etch rate correlated well with other properties such as the refractive index and the mechanical hardness.

4.2. Particle Size Dependence. The particle size dependence of the etch rate was given in Figure 4. Before we discuss the physical origin of this effect, the implications for the particle size decrease observed during etching (Figure 3) are discussed. It was already noted that a simple cube-root dependence of the diameter on the amount of ZnO present cannot describe the experimental results. An evident improvement would be to include a size dependence and to allow for polydispersity. This was done in the following way.

The etching was simulated in a Monte Carlo process. The rate of etching was translated into the probability that a particular particle would lose one ZnO unit. Thus, approximately 1000 etch steps are necessary to completely dissolve a 36 Å ZnO particle (1000 units). The experimental data were used to estimate a dependence on size D. The dashed lines in Figure 4 show models using an exponential [exp(1/D)] and a power (D^{-5}) relationship. The degree of polydispersity was varied between zero and the value found from TEM size histograms,[4] (approximately 70% of the particles have a diameter within 10−15% of the average). At appropriate intervals during the etch simulation, the volume-weighted average diameter (this is the quantity obtained from absorption measurements[4]), the number of particles, and the degree of polydispersity were calculated.

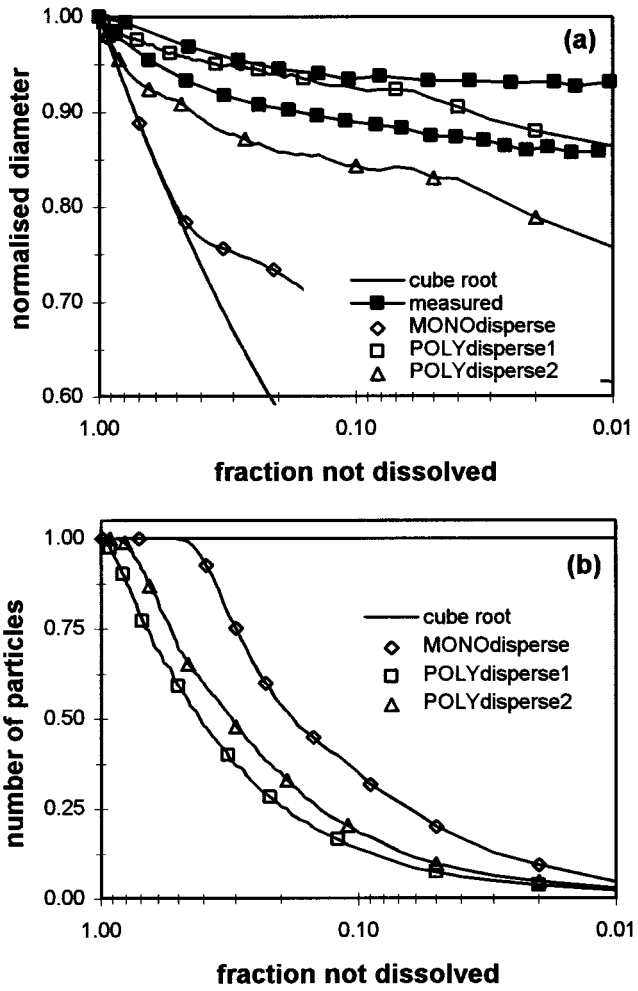

Figure 7. Monte Carlo simulations of ZnO etching. (a) and (b) show the normalized volume-weighted diameter and the normalized number of particles, respectively. Note the logarithmic *x*-axis describing the fraction of ZnO not dissolved. The open symbols refer to simulations using 200 particles of 1000 ZnO units. Closed symbols in (a) are two sets of measured data (identical to Figure 3). The solid line describes the cube-root dependence.

Some typical results based on the experimentally found size dependence are collected in Figure 7a,b. They were obtained by averaging a number (typically 5) of simulations using a set of 200 particles of 1000 ZnO units. The shape of the curves and the effects of the polydispersity and the size dependence were very similar to what was found using other sets of ZnO particles. "POLYdisperse1" represents a Gaussian size distribution with a degree of polydispersity similar to that found experimentally;[4] "POLYdisperse 2" has half the width of POLYdisperse1. Note the logarithmic *x*-axis which is identical to that in Figure 3. Figure 7a shows the normalized volume-weighted diameter. The solid line indicates the simple cube-root dependence. Two sets of experimental results are included as filled symbols. Figure 7b shows the normalized total number of particles left.

The main feature of the experimental data was the small size decrease, which levels off while etching progresses. Simulations were aimed at reproducing this. If no size dependence was taken into account or if a monodisperse set of particles was used, an excessive size decrease during etching was invariably found. The curve for MONOdisperse in Figure 7a illustrates this point for a strong size dependence. Thus, both polydispersity *and* a pronounced size dependence have to be included in the simulations. The curves labeled POLYdisperse in Figure 7a were obtained in this way. The exponential dependence and

the power dependence of the etch rate on size (see Figure 4) gave virtually identical results. They show good agreement with the experiments, except for the final stage of etching (<5% ZnO left).

It is possible to get a closer match between simulation and experiment by adjustment of the degree and the nature (Gauss, Poisson, arbitrary) of the particle-size distribution and the size dependence. However, this is of little value because no unique fit can be obtained and because of some uncertainties in the model. The experimentally determined size dependence need not be valid down to zero size. Second, the total volume of ZnO is measured by the absorption at 300 nm (A_{300}), as outlined in Results. This is a good assumption down to approximately 2 nm particle size. For smaller sizes no data are available. It is, therefore, possible that the measurements underestimate the number of very small particles present during etching. The effect on the calculated particle size is relatively small, however, because this is a volume-weighted quantity.

The degree of polydispersity increased slightly in all the simulated etch experiments. This is in accordance with the experimental data. The degree of polydispersity clearly has a significant effect on the eventual size decrease. Therefore, the small differences in the size evolution observed experimentally are ascribed to small variations of the polydispersity between sols.

It is concluded that the evolution of the particle size during etching can be understood on a semiquantitative level as a random process, which incorporates a size dependence and polydispersity that are in good agreement with experimental data. Due to the polydispersity, smaller particles are invariably present. These are etched quickly, while larger particles remain relatively unaffected. Hence, the number of particles decreases soon after the start of the etching, as seen in Figure 7b, and the volume-weighted size decreases only slowly.

On the basis of experiments on the competitive dissolution of a mixture of sols, (see Figure 5), it was concluded that the size dependence of the etch rate was not due to variations of factors such as pH or ionic strength. The close agreement between the simulated and the measured size evolution, provided that the size dependence is included, lends further support to this conclusion as all particles in a single sol experience the same chemical environment.

Some attempts have been made in the literature to model the etching of small silica particles. Polydispersity was not taken into account in these works. The etch rate was proportional to the available surface area at all times during the etch process in the case of particles larger than 0.1 μm.[10] Such a model could not be applied to smaller particles and also failed here. Iler described the dissolution of much smaller silica particles in dilute alkaline solution.[11] The dissolution rate of 1.85 nm particles was >20 times faster than that of 3.3 nm particles. Obviously, the etch rate does not scale with the fraction of atoms located at the surface, and additional effects are involved. Such a marked size dependence could also not be explained by models based on enhanced solubility of small particles according to the Kelvin equation.[11]

The same conclusions apply to the size dependence found here. Moreover, the Monte Carlo simulations and etch experiments on a mixture of sols are consistent with the same size dependence. Variations of pH, concentrations of solute species, etc., can therefore be excluded as possible causes, in contrast to other work.[11] The rate-determining step in the etching of single-crystal ZnO[9] was argued to be the hydrolysis of ZnO units at kink sites. The number of such active sites depends strongly on the curvature and the surface morphology of nanoparticles. One can also imagine that the defect concentration goes down as the particle size increases.

Thus, the strong size dependence found for the etch rate of ZnO nanoparticles is interpreted as evidence for large differences in the chemical reactivity. This is analogous to the kind of size selectivity through reactivity mentioned before.[7] However, we have not been able to enhance the monodispersity of a single sol in this way, probably because the selectivity is not strong enough. It would be interesting to study the size dependence and possible size selectivity of the dissolution of other nanoparticles. Suitable candidates may be capped Au and CdSe nanocrystallites because modulation of their size has been demonstrated by variation of the concentration of the capping agents (surfactants).[14]

5. Conclusions

Addition of acid can be used to slowly etch ZnO nanoparticles in ethanolic solution. The average particle size decreases. A strong size dependence of the etch rate is found. The evolution of the size of the particles during etching can be described by a random process if the size dependence of the etch rate and the degree of polydispersity are taken into account correctly. The absolute value of the etch rate varies between ZnO sols produced in different synthesis runs.

Comparison with work on silica nanoparticles and etching of ZnO single crystals points out that differences in chemical reactivity are the most probable cause of these observations. Such differences should be taken into account when other properties, such as luminescence or electrical conductivity, are studied. Thus, the dissolution of ZnO nanoparticles in ethanolic solution provides a convenient method to investigate size-dependent properties. It would be interesting to extend this approach to other nanoparticle systems of well-defined size and polydispersity, and to look for other manifestations of variations in the chemical reactivity.

References and Notes

(1) O'Regan, B.; Grätzel, M. *Nature* **1991**, *353*, 737.
(2) Gupta, T. K. *J. Am. Ceram. Soc*. **1990**, *73*, 1817; Chopra, K. L.; Major, S.; Pandya, D. K. *Thin Solid Films* **1983**, *102*, 1.
(3) Koch, U.; Fojtik, A.; Weller, H.; Henglein, A. *Chem. Phys. Lett*. **1985**, *122*, 507.
(4) Meulenkamp, E. A. *J. Phys. Chem*. **1998**, *102*, 5566.
(5) van Dijken, A.; Vanmaekelbergh, D.; Meijerink, A. *Chem. Phys. Lett*. **1997,** *269*, 494; van Dijken, A.; Janssen, A. H.; Smitsmans, M. H. P.; Vanmaekelbergh, D.; Meijerink, A. *Chem. Mater*. **1998**, in press.
(6) Matsumoto, H.; Sakata, T.; Mori, H.; Yoneyama, H. *Chem. Lett*. **1995,** 595; *J. Phys. Chem*. **1996**, *100*, 13781.
(7) Whetten, R. L. *Mater. Sci. Eng*. **1993**, *B19*, 8.
(8) Spanhel, L.; Anderson, M. A. *J. Am. Chem. Soc*. **1991**, *113*, 2826.
(9) Gerischer, H.; Sorg, N. *Electrochim. Acta* **1992**, *37*, 827.
(10) O'Connor, T. L.; Greenberg, S. A. *J. Phys. Chem*. **1958**, *62*, 1195.
(11) Iler, R. K. *The chemistry of silica—solubility, polymerization, colloid and surface properties, and biochemistry*; John Wiley & Sons: New York, 1979.
(12) Mićić, O. I.; Sprague, J.; Lu, Z.; Nozik, A. J. *Appl. Phys. Lett*. **1996**, *68*, 3150.
(13) Maekawa, S.; Ohishi, T. *J. Non-Cryst. Solids* **1994**, *169*, 207; Bernards, T. N. M.; Huls, B. G.; van Bommel, M. J. *J. Sol-Gel Sci. Technol*. **1997**, *10*, 193.
(14) Platschek, V.; Schmidt, T.; Lerch, M.; Müller, G.; Spanhel, L.; Emmerling, A.; Fricke, J.; Foitzik, A. H.; Langer, E. *Ber. Bunsen-Ges. Phys. Chem*. **1998**, *102*, 85; Leff, D. V.; Ohara, P. C.; Heath, J. R.; Gelbart, W. M. *J. Phys. Chem*. **1995**, *99*, 7036.